



HAL
open science

Qualification and post-mortem investigation of actively cooled tungsten flat-tile mock-ups for WEST divertor

Marc Missirlian, G. Pintsuk, G.-N. Luo, Q. Li, W. Wang, A. Durif, T. Batal, M. Richou, J. Bucalossi

► To cite this version:

Marc Missirlian, G. Pintsuk, G.-N. Luo, Q. Li, W. Wang, et al.. Qualification and post-mortem investigation of actively cooled tungsten flat-tile mock-ups for WEST divertor. *Fusion Engineering and Design*, 2018, 136, pp.403-409. 10.1016/j.fusengdes.2018.02.063 . cea-04724777

HAL Id: cea-04724777

<https://cea.hal.science/cea-04724777v1>

Submitted on 7 Nov 2024

HAL is a multi-disciplinary open access archive for the deposit and dissemination of scientific research documents, whether they are published or not. The documents may come from teaching and research institutions in France or abroad, or from public or private research centers.

L'archive ouverte pluridisciplinaire **HAL**, est destinée au dépôt et à la diffusion de documents scientifiques de niveau recherche, publiés ou non, émanant des établissements d'enseignement et de recherche français ou étrangers, des laboratoires publics ou privés.

Qualification and Post-mortem Investigation of actively cooled Tungsten flat-tile mock-ups for WEST divertor

M. Missirlian^{a*}, G. Pintsuk^b, G.-N. Luo^c, Q. Li^c, W. Wang^c, A. Durif^a, T. Batal^a,
M. Richou^a, J. Bucalossi^a

^a CEA, IRFM, F-13108 Saint-Paul-Lez-Durance, France

^b Forschungszentrum Jülich GmbH, Institut für Energie- und Klimaforschung – Plasmaphysik, Partner of the Trilateral Euregio Cluster (TEC), 52425 Jülich, Germany

^c Institute of Plasma Physics, Chinese Academy of Sciences (ASIPP), Hefei, Anhui, China

The WEST (W -for tungsten- Environment in Steady-state Tokamak) project has provided the opportunity of to developing and qualifying, in collaboration with ASIPP (China) and FZJ (Germany) a newly attractive W/Cu actively cooled PFCs technology able to sustain high heat loads close to ITER divertor ones.

Within this framework, ASIPP has produced two small-scale mock-ups based on the W-armoured flat-tile concept. The results presented herein focus on the qualification program, performed by CEA, which consisted in a preliminary non-destructive testing (NDT) control based on infrared thermography to assess the joint interface quality followed by cyclic high heat flux (HHF) testing performed at FZJ. The HHF testing, performed by successive thermal cycling, allowed demonstrating the thermal performance of this technology to remove heat loads over several hundreds of cycles at 20 MW/m² without obvious indication of damage impacting the heat exhaust capability for both mock-ups. Furthermore, the subsequent post-mortem microstructural analysis allowed confirming the issues regarding the induced fatigue damages, especially the tungsten crack formation perpendicular to the incident surface appeared during cycling at 10 MW/m² and plastic deformation inducing microstructure evolution in the pure Cu-interlayer during cycling beyond 10 MW/m² for both mock ups.

Keywords: tungsten armored actively cooled components, flat-tile concept, HHF testing

1. Introduction

The WEST (W -for tungsten- Environment in Steady-state Tokamak) tokamak, which is operational since end of 2016, is based on an upgrade of the Tore Supra machine [1, 2]. It consists in implementing an actively cooled tungsten divertor for testing high heat flux technology under tokamak conditions [3]. Beside the ITER divertor technology (i.e. W-monoblock), presently tested during the WEST experimental campaigns, the WEST team has also devoted time, in collaboration with ASIPP (China) [4], into the development and the qualification of other attractive W/Cu actively cooled plasma facing components (PFCs) able to sustain heat loads close to ITER divertor ones. This contribution presents the main outcome obtained on mock-ups based on W flat-tile technology which have been produced in the frame of this collaboration. The pre-examination including the infrared thermography inspection to control the bonding quality after manufacturing phase, as well as the high heat flux experimental campaign performed in the electron beam facility JUDITH-1 (FZ-Jülich, Germany) [5] to assess the thermal performance are commented and the subsequent post-mortem multi-scale microstructural analysis are discussed. The most important issues regarding the induced fatigue damages are hence investigated, especially the brittleness of tungsten being prone to crack formation and plastic deformation inducing changes in the pure Cu-interlayer.

2. Manufacturing of W flat-tile mock-ups

In 2015, ASIPP manufactured two small-scale W/Cu flat-tile mock-ups for CEA's WEST project. The two W flat-tile mock-ups, marked as FT-1 and FT-2, were manufactured firstly by casting of oxygen free copper (OFC-Cu) onto the rear side of W tiles (the rolling direction of W tiles being set perpendicular to the plasma facing surface), followed by HIPing of W/OFC-Cu tiles onto CuCrZr heat sink plate [6]. Each mock-up, with a dimension of 84 mm (length) x 30 mm (width) x 17 mm (height), consisted in 7 tungsten tiles (length of 12 mm, thickness of 2 mm) bonded on the CuCrZr heat sink with a cooling channel of 8 mm in diameter drilled in it (see figure 1). It is 6 mm thick between the top of the cooling channel and the surface of mock-ups.

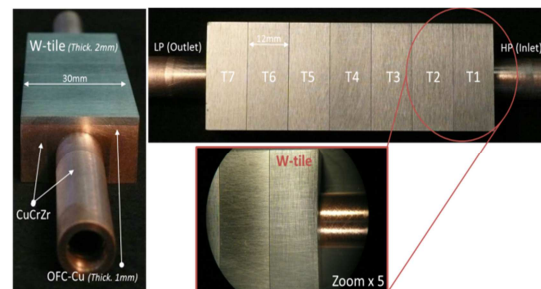


Fig. 1. Different views of W/Cu flat-tile test mock-up

3. Testing program

The qualification program of actively cooled components for WEST includes several tests. The high heat flux (HHF) thermal fatigue testing is the leading part of the qualification. This testing enables

to check the robustness of the PFC under thermal exposure as close as possible to those foreseen during WEST plasma in nominal conditions (namely, up to 10 MW/m^2) and beyond, to evaluate the limit of design and to obtain information on the components thermal fatigue lifetime. In addition, the thermal fatigue testing is preceded and then followed by a dedicated non-destructive examination. Based on a visual control and an active infrared thermography inspection, the non-destructive examination enables to check the manufacturing quality prior to thermal fatigue testing (pre-examination) and to assess the damage evolution (post-examination) which supports a better understanding of the thermal behaviour.

3.1 Infrared thermography inspection

A well-established facility named SATIR (French acronym for infrared acquisition and data processing device [7]), used at CEA (Cadarache, France) these last years for W-armoured actively cooled components [8] in the frame of studies dedicated to mock-ups/prototypes for ITER divertor, has proved to be very efficient for detecting and qualifying potential imperfection in terms of the heat removal capability of high heat flux components. This technique is based on the detection of a time delay of the surface temperature evolution measured by IR thermography during a fast decrease of the water temperature flowing in the cooling tube. An imperfection at one of the joints or in material creates a thermal resistance so that the time response delay increases during the transient thermal regime. This delay is measured by comparison with the thermal behavior of a 'defect-free' reference component (or tile). The maximum value of this delay in terms of temperature –called DT_{ref_max} ($^{\circ}\text{C}$)– is calculated for each pixel on the IR images. The emissivity variations in surface are corrected by processing based on a pixel normalization algorithm during the hot thermalization (hot water flow at $\sim 100^{\circ}\text{C}$ into the cooling tube) for steady-state conditions at the beginning of test [9]. This technique was applied on each W flat-tile mock-up.

3.2. Thermal fatigue testing

HHF thermal fatigue tests were carried out to assess the performance of W flat-tile technology under cyclic heat load by means of electron beam facility JUDITH-1. The cooling water conditions were inlet velocity of 10 m/s, inlet temperature of 20°C and inlet pressure of 22.5 bars. The monitoring of the thermal loads was provided by means of a CCD camera, two-color pyrometer and an IR camera. The absorbed heat flux is obtained by a global calorimetry from the averaged measurement of three thermocouples installed at the inlet as well as the outlet of the tested components. The experimental campaign was devoted to several steps of fatigue cycle tests (see table 1). The reduction in loaded number of tiles with increasing power density is owed to the limitation of the available beam power. The thermal cycle was 10 s power on, then 10 s dwell time. Initial, intermediate

and final screenings (thermal mapping) were performed at 5 MW/m^2 between the cycling phases. Due to the lack of a calibration tile, the emissivity calibration was done in-situ during screening at the particular power density via cross referencing two-color pyrometer data with those of the IR-camera. This calibration is performed also for intermediate cycles to check the influence of a decreasing transmission efficiency of the observation windows due to surface coating from the inside by evaporated species from the component.

Table 1. Planned test scheme
(*cycle=10 s ON / 10 s OFF; screening ~60-120 s*)

FT-1		
# of cycles	Power density (MW/m^2)	Heat loaded tiles
100	10	Tiles 2 to 6
100	15	Tiles 3 to 5
300	20	Tiles 3 to 5
FT-2		
# of cycles	Power density (MW/m^2)	Heat loaded tiles
300	10	Tiles 2 to 6
100	15	Tiles 3 to 5
100	20	Tiles 3 to 5

4. Results and discussion

4.1. Infrared thermography inspection

The SATIR quality criterion is based on previous results [10] related to a comprehensive study to define acceptance criteria for the divertor PFCs with regards to thermomechanical fatigue. This study confirmed that the most critical part of a PFC is the armour-to-heat-sink joint and proved that the dimension of defect extension at the interfaces of bonding was a relevant criterion. It was finally stated that the maximum acceptable defect dimension independent of the location is about 20% of the joint surface for the flat-tile geometry. Thereafter, based on finite element calculations, the extrapolation to the W flat-tile components considered in this study leads to a 'faulty tile' threshold in terms of DT_{ref_max} of 6°C , the detectability threshold of the SATIR device being 4°C .

Figure 2 shows the SATIR results (i.e. DT_{ref_max} cartography) obtained on each tile of the FT-1 and FT-2 mock-ups. DT_{ref_max} measurements are assessed by infrared means during the thermal shock between a reference tile (here tile #2) and each region of interest (namely, each W tile). Considering the low DT_{ref_max} measured on each tile of each mock-up, in particular below the 'faulty tile' threshold of 6°C , there is no evidence of abnormal heat transfer capability of the components. This result points out the good manufacturing quality (particularly, the good bonding of W/Cu and Cu/CuCrZr joints) prior to thermal fatigue testing.

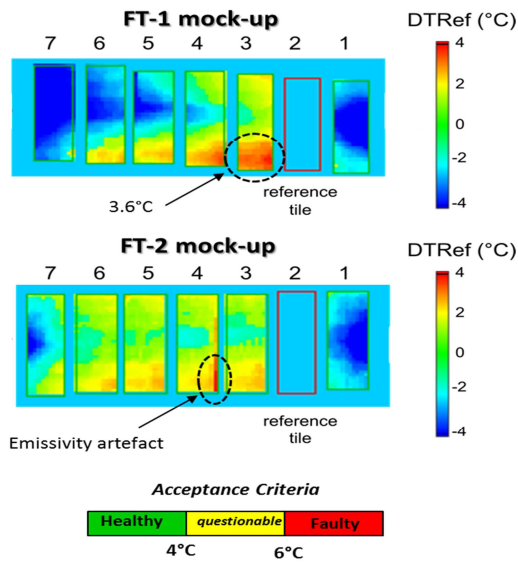


Fig. 2. SATIR results for FT-1 and FT-2 mock-ups before HHF testing

4.2. Thermal fatigue testing

The IR-images (for emissivity (ϵ) assessed to 0.18) at the first (so-called before cycling) and last (so-called after cycling) cycle for each step of heat loads for each mock-up are shown in figures 3 to 5. The IR-images indicate that no significant degradation of the heat removal capability of each tested component and in particular no local hot spot was observed during the thermal cycling. In addition, the cool down behavior for the most highly loaded tiles (#3, #4 and #5) before and after cycling at 20 MW/m² is plotted in figure 6 for each mock-up. As no clear difference in cool down behavior between before (i.e. the first cycle) and after (i.e. the last cycle) cycling is noted, one can say that no degradation of the cool down performance took place.

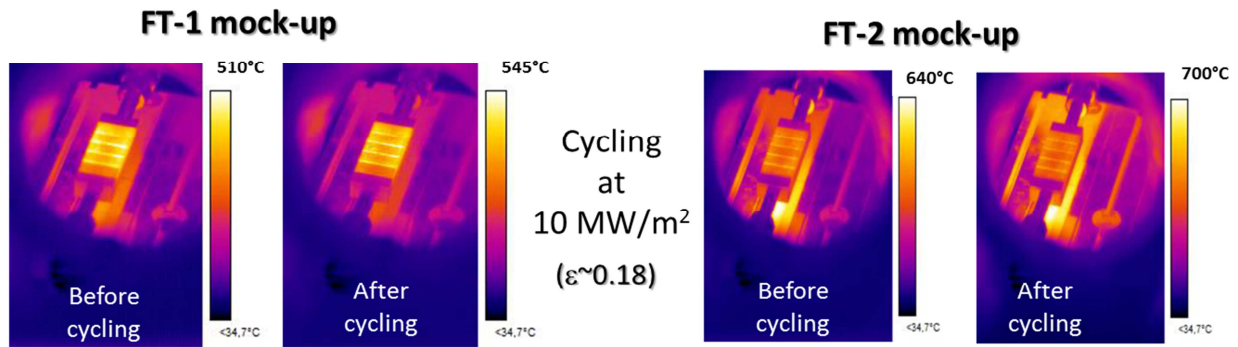


Fig. 3. IR-images of FT-1 and FT-2 mock-ups during the first and the last cycles at 10 MW/m²

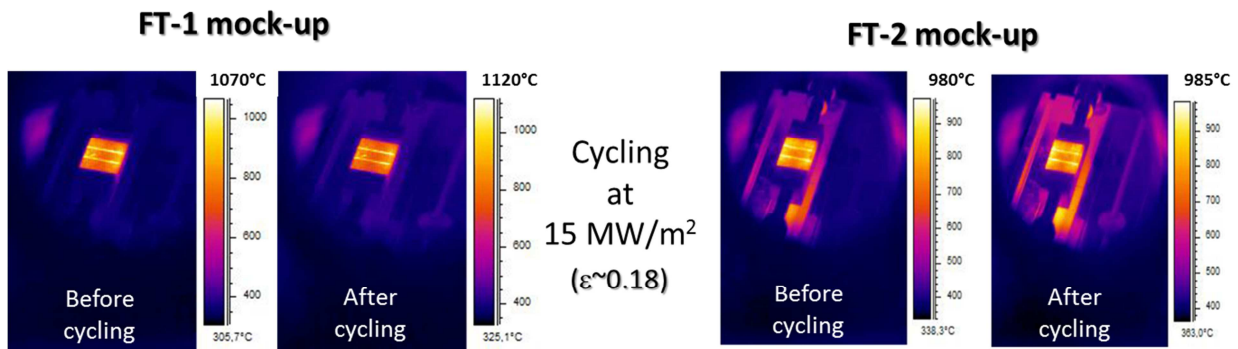


Fig. 4. IR-images of FT-1 and FT-2 mock-ups during the first and the last cycles at 15 MW/m²

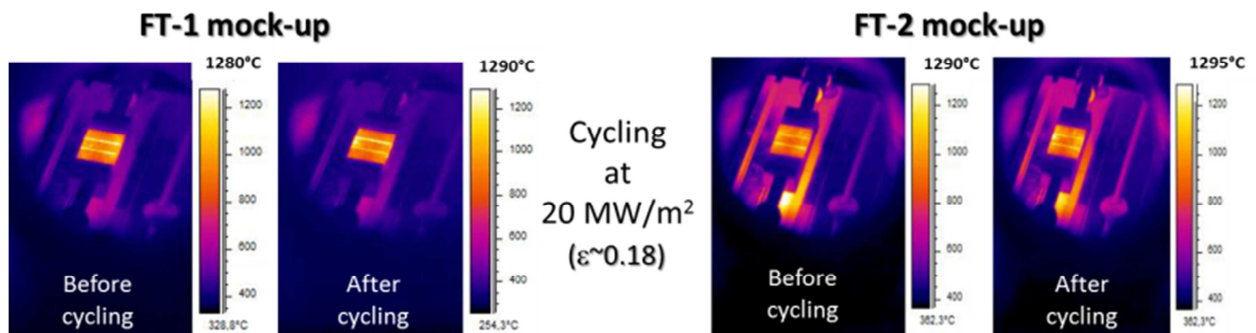


Fig. 5. IR-images of FT-1 and FT-2 mock-ups during the first and the last cycles at 20 MW/m²

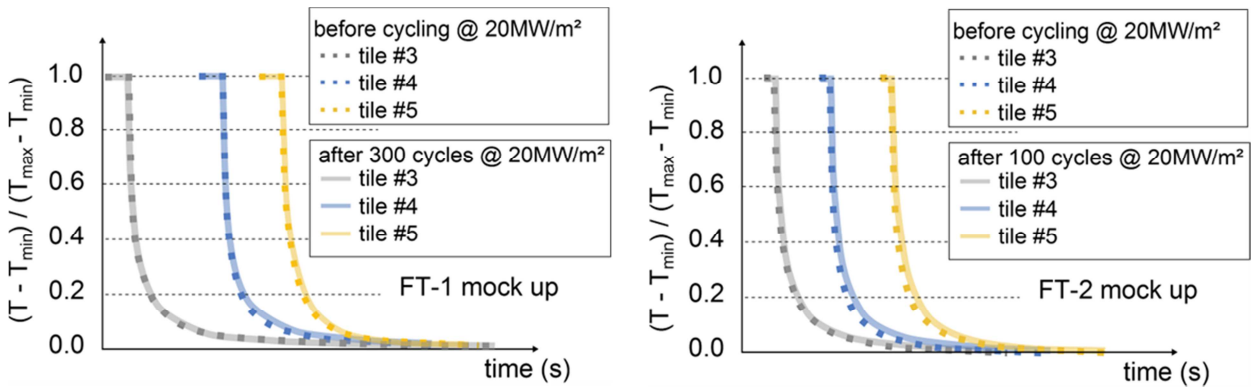


Fig. 6. Cool down performance measurement (based on normalized temperatures) in arbitrary units (a.u) before and after cycling at 20 MW/m² for FT-1 and FT-2 mock-ups

However, while from two-color pyrometer and the IR-camera measurements no degradation of the thermal performance of the tile has been observed, visual inspection on both mock-ups tested up to 20 MW/m², showed a strong deformation of Cu interlayer with an extrusion of Cu (see figure 7).

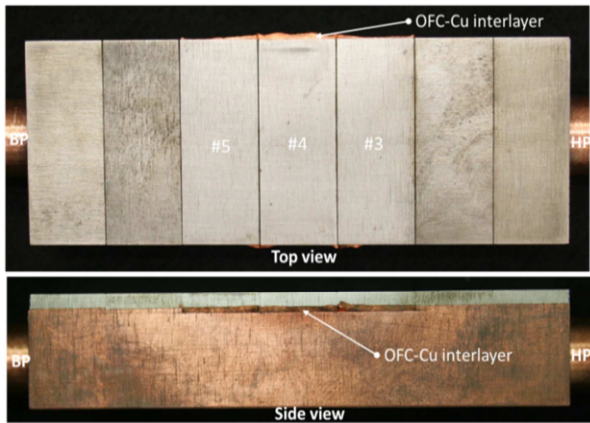


Fig. 7. Illustration: OFC-Cu deformation (extrusion) observed on tiles #3 to #5 for FT-1 mock-up

Cycling at 10 MW/m² as a potential cause for this strong deformation can be excluded since deformation of the copper interlayer occurs only below tiles #3, #4 and #5.

FEM calculation of figure 8 (for HHF hydraulic conditions) shows temperature distribution (for 20 MW/m² heat load) up to ~1140°C on tungsten surface and corresponding temperatures in the pure Cu interlayer up to ~750°C. These high temperatures in Cu, combined with high thermal stresses (i.e. high plastic strain, typically above 2.5%), may be the explanation for the observed strong deformation by creeping of the Cu-interlayer in both mock-ups. However, as no obvious degradation of the thermal performance of both mock-ups was observed during the thermal cycling at different loading steps (as shown previously in figure 6), it can be concluded that this deformation of the pure copper interlayer hardly impacted the heat removal capability of W/Cu flat-tile tested mock-ups.

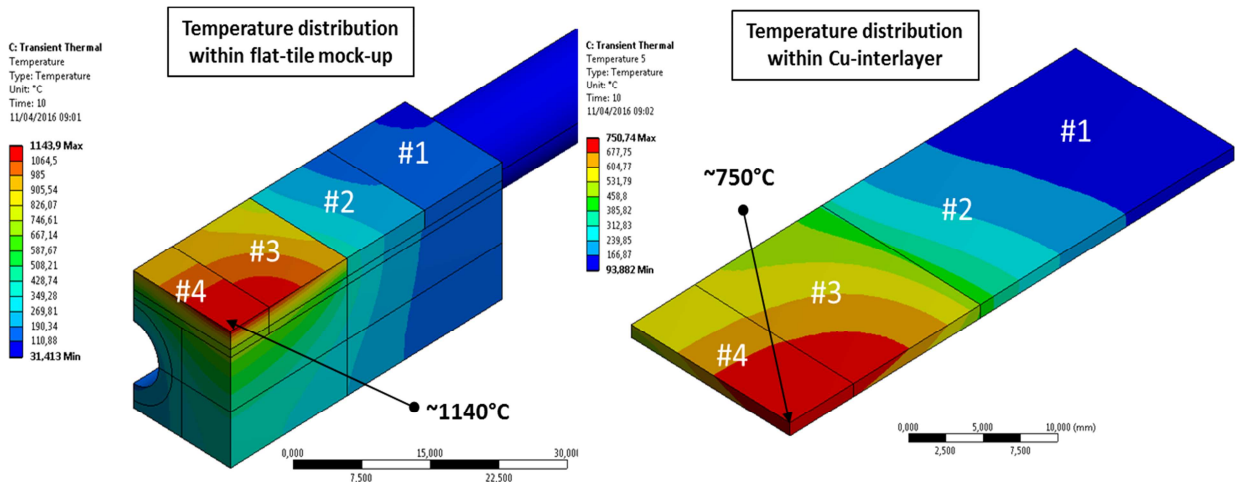


Fig. 8. Thermal 3D-FEM calculation: Temperature distribution within flat-tile mock-up after 10s at 20 MW/m² on tile #4

4.3. Post-mortem metallographic examination

Metallographic analyses have been performed for each mock-up on tile #1 (not heat loaded), tile #2 (loaded only at 10 MW/m²) and a tile loaded up to 20 MW/m² (namely, tile #4 and tile #5 for FT-1 and FT-2 mock-up, respectively).

Global optical micrographs taken from tile #1 do not reveal any crack or major defect for each mock-up, while for tiles #2, #4 and #5 cracks in tungsten are observed oriented perpendicularly to the incident surface (i.e. parallel to the heat flux direction following tungsten microstructure orientation). Concerning tile #2 (loaded only at 10 MW/m²) these cracks propagate from the loading surface to the middle of the tungsten tile, while for tiles #4 for FT-1 and #5 for FT-2 (loaded up to 20 MW/m²), these cracks propagate from the loading surface till inside the OFC-Cu interlayer (see figure 9-left). Optical micrographs revealed mixed propagation into the W material with cracks growing along trans-granular and inter-granular path. SEM analysis performed on tile #5 to observe more precisely the fracture surfaces into the tungsten (see figure 9-right) shows brittle cleavage fracture with several trademarks (i.e. ‘river pattern’). These white lines display how the grains (crystals) have splintered during the cracking. However, as these cracks are oriented perpendicularly to the incident surface into the W material and are still growing randomly into the Cu-interlayer for tiles tested up to 20 MW/m² (most notably with small extension due to a recent occurrence because of low thermal cycling), it does not affect the heat exhaust capacity of the component and induces probably a stress releasing effect.

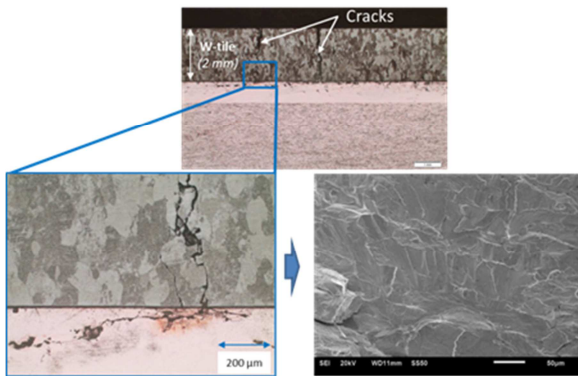


Fig. 9. Crack propagation observed by optical micrographs (*left*) and fracture surface obtained by SEM analysis (*right*) for tile #5 of FT-2 mock-up

Additionally, optical micrographs point out OFC-Cu plastic flow (see figure 10) and damage at the W/Cu interface for tile #4 (for FT-1 mock-up) and tile #5 (for FT-2 mock-up). The plastic flow observed on tile #4 for FT-1 is stronger than on tile #5 for FT-2 due to stiffer solicitations at 20 MW/m² (300 cycles for FT-1 to be compared with 100 cycles for FT-2). Comparing optical micrographs obtained for tiles #1, #2 for each mock-up and #4 (for FT-1 mock-up) or #5 (for FT-2 mock-up), we can observe a change of the OFC-Cu microstructure (grain refinement - see figure 11). Concerning tiles #1 and #2 the grain size is

millimetric while for tiles #4 and #5 grain size is micrometric. The microstructure evolution (i.e. the grain refinement) as well as the plastic flow observed on tiles #4 and #5 confirms that OFC-Cu interlayer reached high temperature combined to high thermal stress during the thermal cycling up to 20 MW/m².

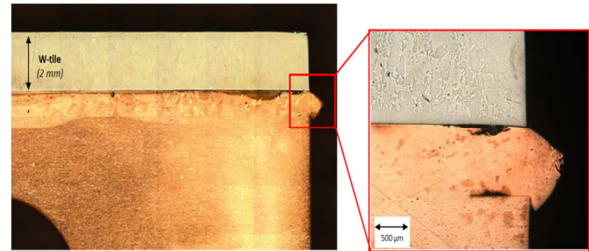


Fig. 10. Optical micrograph observation: Plastic flow on the tile #4 for FT-1 mock-up

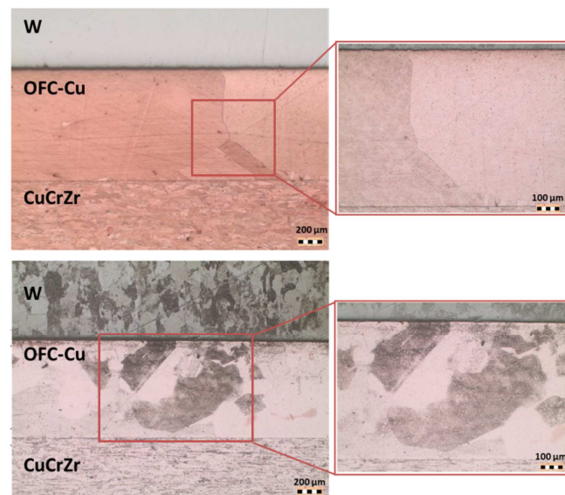


Fig. 11. Optical micrograph observation: Grain refinement between tile #1 (*top*) and tile #5 (*down*) for FT-2 mock-up

5. Summary

Thermal performance of two mock-ups (FT-1 and FT-2) based on W/Cu actively cooled flat-tile technology was investigated. The associated qualification program consisted in a preliminary non-destructive testing (NDT) control based on infrared thermography (through SATIR facility) to assess the joint interface quality followed by cyclic high heat flux (HHF) testing in the electron beam facility JUDITH-1 (FZ-Jülich).

The SATIR results pointed out the good manufacturing quality prior to thermal fatigue testing, and the HHF testing, performed by successive thermal cycling at 10 MW/m², 15 MW/m² then 20 MW/m², allowed demonstrating the thermal performance of this technology to remove heat loads over several hundreds of cycles at 20 MW/m² without obvious indication of damage impacting the heat exhaust capability for both mock-ups. Indeed, despite cracks perpendicular to the incident surface, which appeared during cycling at 10 MW/m² and a clear deformation with an extrusion of Cu interlayer during

cycling beyond 10 MW/m² for both mock ups, no obvious surface temperature increase was observed during thermal cycling.

Furthermore, the subsequent post-mortem microstructural analysis allowed confirming these issues regarding the induced fatigue damages, especially the tungsten crack and plastic deformation inducing microstructure evolution in the pure Cu-interlayer.

References

- [1] J. Bucalossi et al. Fusion Eng. Des. 86 (2011) 684-688
- [2] J. Bucalossi et al. Fusion Eng. Des. 89 (2014) 907-912
- [3] M. Missirlan et al. Fusion Eng. Des. 89 (2014) 1048-53
- [4] G.N. Luo et al. Nucl. Fusion 57 (2017) 065001 (9pp)
- [5] R. Duwe et al. Fus Tech. 27 (1995) 356-358
- [6] Q. Li et al. Phys. Scr. T170 (2017) 014020 (10pp)
- [7] A. Durocher et al. Nuclear Fusion 47 (2007) 1682-89
- [8] M. Missirlan et al. Phys. Scr. T145 (2011) 014080
- [9] N. Vignal et al. Fusion Eng. Des. 88 (2013) 1818-22
- [10] F. Escourbiac et al. Phys. Scr. T138 (2009) 41047588